Wear 486–487 (2021) 204085

Contents lists available at ScienceDirect

Wear

journal homepage: www.elsevier.com/locate/wear

Mechanism of oil-lubrication of PEEK and its composites with steel counterparts

Go Tatsumi [a,b,*], Monica Ratoi [a], Yuji Shitara [b], Shinji Hasegawa [b], Kiyomi Sakamoto [b], Brian G. Mellor [c]

[a] National Centre for Advanced Tribology at Southampton (nCATS), University of Southampton, Southampton, SO17 1BJ, United Kingdom
[b] Lubricant R&D Dept., ENEOS Corporation, 8, Chidoricho, Naka-ku, Yokohama, 231-0815, Japan
[c] Faculty of Engineering and Physical Sciences, University of Southampton, Southampton, SO17 1BJ, United Kingdom

ARTICLE INFO

Keywords:
Polyetheretherketone (PEEK)
Carbon fiber reinforced (CFR) PEEK
Glass fiber reinforced (GFR) PEEK
Polymer transfer film
Boundary lubrication
Sliding-rolling contact

ABSTRACT

The rapid adoption of the advantageous PEEK and its composites paired with steel counterparts in many tribological applications has prompted intense research to investigate their tribological properties under lubrication. This study investigated the effect of oil-lubrication and proposed a mechanism of action. Compared to the dry conditions, oil-lubrication with poly-α-olefin (PAO) base oils reduced friction, regardless of the type of polymer materials. However, the wear behavior depended on the polymer type; it increased for neat PEEK and decreased for PEEK composites. Additionally, the viscosity of the lubricant oils influenced the polymer behavior in distinct ways. These differences in tribological performance under oil-lubrication were explained by two important factors, the polymer transfer films on steel counterparts determined by Electron Probe Micro Analysis (EPMA) and the hardness modification of the polymer surfaces investigated by nanoindentation measurements. These factors were also related to each other, especially for PEEK composites.

1. Introduction

Polymers and polymer-based composites are often used in diverse tribological parts such as gears, bearings, bushings and seals in the automotive, aerospace and medical sectors. Compared to metals, they are lighter, less noisy and have self-lubricating properties [1–6]. Due to their self-lubricating properties polymers are commonly used with steel counterparts in dry conditions, and this has been the object of numerous studies on their friction and wear properties [7–14]. However, as polymers have lower mechanical strength and thermal stability than metals failure can result from wear, local melting and pitting when used under severe conditions [15–18]. Among the many types of polymers, Poly-Ether-Ether-Ketone (PEEK) has superior mechanical properties and higher thermal stability than other conventional polymers which make it suitable for tribological applications operating under severe conditions [1,2,19,20]. In addition, fiber reinforced PEEK composites such as carbon fiber reinforced (CFR) PEEK and glass fiber reinforced (GFR) PEEK are also widely applied due to their improved mechanical properties [3,21,22].

While fillers such as PTFE, graphite, MoS_2, and WS_2 have been used to improve the properties of PEEK and its composites [23–29], lubrication with water or oil-based fluids has the potential to improve their tribological properties further [30–38]. Fluid films can separate completely or partially two sliding surfaces and mitigate friction and wear, but little is known about the fluid lubricated contacts of PEEK and its composites compared to dry conditions. Moreover, the reported research showed that fluid lubrication is not always beneficial in polymer-steel contacts and can increase friction and/or wear of PEEK and its composites paired with steel counterparts [33,34,38–41]. This needs to be understood better so that PEEK and PEEK composites can be applied to more systems.

In terms of mechanism of action, two key factors are reported to influence the tribological properties of PEEK and PEEK composites with steel counterparts: polymer transfer films formed on steel counterparts and hardness modification of polymer surfaces. Polymer transfer films on steel counterparts are essential to reducing wear as they act as a protective layer so avoiding the direct contacts between polymer surfaces and the hard asperities of steel counterparts [9,13,42]. It was reported by Kurdi et al. [41] that water lubrication of a PEEK-steel contact led to decreased friction but greatly increased wear of the PEEK

* Corresponding author. National Centre for Advanced Tribology at Southampton (nCATS), University of Southampton, Southampton, SO17 1BJ, United Kingdom.
E-mail address: tatsumi.go@eneos.com (G. Tatsumi).

https://doi.org/10.1016/j.wear.2021.204085
Received 30 March 2021; Received in revised form 2 August 2021; Accepted 30 August 2021
Available online 3 September 2021

compared with dry conditions. This was ascribed to water inhibiting the formation of stable transfer films on steel counterparts. On the other hand, Zhang et al. [33] found that lubrication with diesel fuel reduced friction and wear of PEEK with steel counterparts and the presence of a polymer transfer film on the steel was observed. However, no polymer transfer film was observed for the PEEK composite containing multiple fillers of carbon fibers, solid lubricants, and ceramic particles, causing higher friction and wear of the PEEK composite compared to neat PEEK. The second key factor, the hardness modification of polymer surfaces, was investigated by Yamamoto and Takashima [39] who showed that water lubrication of a PEEK-steel contact increased the wear of PEEK dramatically compared with the dry condition. The hardness of the rubbing surface of PEEK was decreased during the water lubricated test, which made the authors postulate that this softening caused the high wear of PEEK. This was also observed in water lubricated conditions by Yamaguchi and Hokkirigawa [43]. For PEEK composites, Chen et al. [32] reported that with sea water lubrication of PEEK composites containing carbon fibers and steel counterparts, the exposed fibers on the wear track carried most of the applied contact load and protected the PEEK matrix from severe wear. In contrast, the carbon fibers were crushed and fractured at higher loads, decreasing the load carrying capacity of the composite and causing increased wear. However, the two key factors mentioned above have been investigated mostly with water lubrication and their effect and mechanism of action are still unclear with the oil-lubrication, commonly used for many tribological components.

Therefore, the current study aimed to investigate the effect of oil-lubrication on the tribological properties of neat PEEK and its CFR and GFR composites with steel counterparts, and thus elucidate their working mechanism, essential to developing ideally suited PEEK-based systems for tribological applications. The friction and wear properties were studied under dry and poly-α-olefins (PAOs) lubricated conditions in sliding-rolling contact motion as encountered in gear applications. The working mechanism was further investigated by focusing on two important factors that influence tribological properties, the polymer transfer films on steel counterparts and the hardness modification of polymer surfaces during tribological testing. The effect of fluid viscosity, which is significantly lower for water than oils was specifically addressed by using PAOs with different viscosity grades.

2. Experimental methods

2.1. Materials

Polymer plate specimens 40 × 40 × 2 mm of neat PEEK, CFR PEEK and GFR PEEK were injection molded from commercially available pelletized materials (Fig. 1(a)). The typical properties of each material, adapted from the supplier's catalogue (https://www.solvay.com/), are summarized in Table 1. The polymer plates had a R_a surface roughness of approximately 0.05 μm for neat PEEK and 0.2 μm for CFR PEEK and GFR PEEK, respectively. Steel balls (AISI 52100) with a diameter of 12.7 mm supplied by PCS instruments Ltd were shot blasted to a R_a surface roughness of approximately 0.5 μm. This roughness value was designed to mirror that of the steel counterpart in the targeted polymer gear applications. Each test used new plates and balls cleaned prior to testing with a hydrocarbon-mix solvent (FASTCLEAN 201, CRC Industries UK Ltd) and isopropanol.

Table 1
The typical properties of polymers used in this study.

	Neat PEEK	CFR PEEK	GFR PEEK
Polymer sources	Solvay® KT-820 NT	Solvay® KT-820 CF30	Solvay® KT-820 GF30
Fibre types	none	Carbon fibre	Glass fibre
Fibre contents	none	30 wt%	30 wt%
Young's modulus	3.8 GPa	22.8 GPa	11.4 GPa
Poisson's ratios	0.33	0.42	0.34

Poly-α-olefin (PAO) base oils with different viscosity grades, PAO2, PAO4 and PAO10 were used as test oils. Table 2 shows the detailed properties of each oil. The pressure-viscosity coefficients of PAOs were calculated from the values of kinematic viscosity [44], and used for the calculation of the oil film thicknesses at the operating condition.

2.2. Tribological tests

A Mini Traction Machine (MTM) from PCS Instruments Ltd. was employed to carry out tribological tests under dry and oil-lubricated conditions, as shown in Fig. 1(b and c). Polymer plates were fixed with a nut on top of a bespoke MTM disc. The testing was performed under a slide-roll ratio (SRR) of 50%, an entrainment speed of 0.5 m/s and an applied load of 50 N for 60 min at ambient temperature (approximately 25 °C). The SRR is defined as the ratio of the sliding speed (u_d - u_b) to the entrainment speed ((u_d + u_b)/2), where u_d and u_b are the speeds of the disc and the ball with respect to the contact. SRRs in actual gears vary depending on the design of the gear teeth, but the 50% SRR applied in this study covers the typical range found in gear applications [45,46]. The entrainment speed of 0.5 m/s is typical of the low to middle speed range envisaged in gear applications, and aims to reliably evaluate the wear performance. The maximum Hertzian contact pressure (P_{max}) of the steel ball and polymer plate was calculated as 0.16 GPa in the neat PEEK test, 0.53 GPa in the CFR PEEK test and 0.33 GPa in the GFR PEEK test, respectively. These values of contact pressures were designed to be a higher level compared to previous studies of polymer-steel contacts, because one of the expected advantages of oil-lubrication is to extend the limitation on contact pressures in

Table 2
Typical properties of PAO base oils used in this study.

		PAO2	PAO4	PAO10
Density, g/cm3	15 °C	0.798	0.819	0.836
Kinematic viscosity, cSt	25 °C	8	31	136
	40 °C	5.0	17.5	65.1
	100 °C	1.7	3.9	9.8
Pressure-viscosity coefficient, GPa^{-1}	25 °C	15	19	22

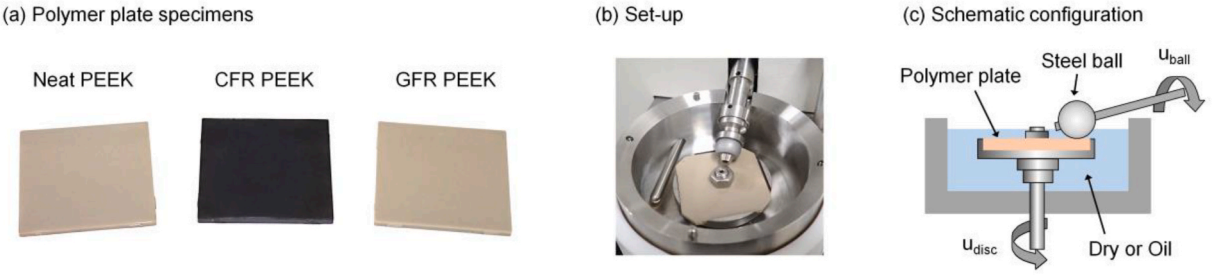

Fig. 1. Appearance of MTM tribometer (a) polymer plate specimens, (b) set-up and (c) schematic configuration.

polymer applications [15].

Friction coefficient values during testing were recorded every 10 s. The wear track profiles of polymer plates were measured with a stylus profilometer (SURFCOM 1500 DX2, Tokyo Seimitsu Co., Ltd.) in four positions (0, 90, 180, 270°) of the circular wear track, followed by the calculation of the average wear volumes. The wear profiles vary slightly depending on their positions on the wear track and the standard deviation is indicated with error bars.

2.3. Surface analyses (EPMA, alicona, nanoindentation)

Electron Probe Micro Analysis (EPMA) was carried out on the wear tracks of the steel balls after tribological tests using a JXA-8530F (JEOL Ltd.). Prior to the surface analyses the after-test specimens were solvent rinsed and dried. EPMA utilizes with Wavelength Dispersive X-ray spectroscopy (WDX) to count the number of X-rays of a specific wavelength diffracted by a crystal. It has higher resolution than Energy Dispersive X-ray spectrometry (EDX) which makes it suitable for carbon mapping. A 15-kV beam at 100 nA current was used for the acquisition of the secondary electron (SE) images and carbon maps.

Wear tracks of polymer plates were investigated with 3D optical profilometers and nanoindentation measurements. 3D surface profiles were generated with an Alicona InfiniteFocus G4 (Alicona Imaging GmbH), with the Focus-Variation technique. An iNano® nanoindenter (NANOMECHANICS, Inc.) equipped with a Berkovich tip was used for nanoindentation measurements. Two methods: continuous stiffness measurement and hardness mapping were used. The hardness of the polymer surfaces as a function of indentation depth was investigated by the continuous stiffness measurement technique [47–49] applying a small, sinusoidally varying signal on top of a DC signal driving the indenter. The hardness at each indentation depth was determined from the response of amplitude and phase. A frequency of 110 Hz and displacement amplitude of 1 nm were used. On the wear tracks of polymer plates sixteen points (4 × 4) at 50 μm intervals were measured under loads of up to 50 mN, target depth of 3 μm and strain rate of 0.01 s^{-1}. The average hardness at each indentation depth was then calculated and given with the error bars representing ± one standard deviation. Hardness mapping was carried out to measure the distribution of reinforcement fibers on the polymer surfaces using a load of 1 mN, target depth of 0.5 μm and strain rate of 1 s^{-1}.6400 points (80 × 80) were indented at 5 μm interval to provide hardness mapping of a 400 × 400 μm area.

3. Results and discussion

3.1. Tribological tests

Friction coefficient values as a function of time under dry and oil lubricated (PAO2, PAO4 and PAO10) conditions are presented in Fig. 2 (a, b, c) for the neat PEEK and PEEK composites. Oil-lubrication significantly reduced friction compared with dry conditions regardless of the polymer material, however, the effect of the viscosity grade of PAO on friction was found to depend on the polymer material. Lower friction was achieved when lubricating neat PEEK with lower viscosity grades PAO and CFR PEEK with higher viscosity grades PAO. The viscosity grades did not make much difference to friction in the GFR PEEK tests, where almost the same friction values were measured with all three PAO oils.

Fig. 3(a–f) summarizes the friction coefficients averaged over the last 10 min of testing and the wear volumes of the polymer plates. The wear volumes (of polymer plates) calculated from the wear profiles in four positions had low values of standard deviations for all tests. In the case of neat PEEK, the dry test showed lower wear than with oil-lubrication. By contrast, CFR and GFR PEEK had much higher wear under dry conditions than oil-lubrication. The different viscosity grades of PAO influenced the friction and wear of polymer plates in specific ways. As such the increase in viscosity increased friction and wear of neat PEEK, it deceased both for CFR PEEK and had almost no effect on GFR PEEK. Under dry conditions, despite their superior mechanical strength resulting from reinforcement fibers, CFR PEEK and GFR PEEK gave larger wear volumes than neat PEEK. This behavior has been reported in previous studies in dry rolling contacts [19,50] where it was suggested that the wear mechanisms were different for neat polymer and polymer composites with fillers.

Images of the steel balls and polymer plates wear tracks are shown in Fig. 4(a–l). The specimens lubricated with PAO2, PAO4 and PAO10 had similar looking wear tracks and therefore only images of the PAO4 specimens, considered representative of all three oils, are shown. Under dry conditions, the wear tracks of the steel balls paired with neat PEEK (Fig. 4(a)) and PEEK composites (Fig. 4(e, i)) looked distinctively different. A polymer transfer film was observed on the wear track of the steel ball paired with neat PEEK. This can explain the very low wear of the neat PEEK plate. By contrast, the wear tracks on the steel balls paired with CFR and GFR PEEK looked polished with barely any polymer transfer film. A large volume of wear debris piled up at the sides of the steel ball wear tracks in the CFR and GFR PEEK tests under dry conditions, suggesting that three-body abrasion by wear debris containing the hard fibers caused the large wear of polymer plates. By contrast, the wear debris of neat PEEK contributed to the formation of polymer transfer films.

The polymer transfer films can also explain the mechanism of action of oil-lubrication. However, in this case it was difficult to compare the polymer transfer films from their appearance (Fig. 4(b, f, j)) and these films were further investigated using EPMA.

3.2. Polymer transfer films on steel balls

Polymer transfer films on steel ball wear tracks were analyzed using EPMA. Fig. 5(a–l) shows Secondary Electron (SE) images of all balls at the end of test. When lubricated with PAO2 and PAO4 polymer transfer

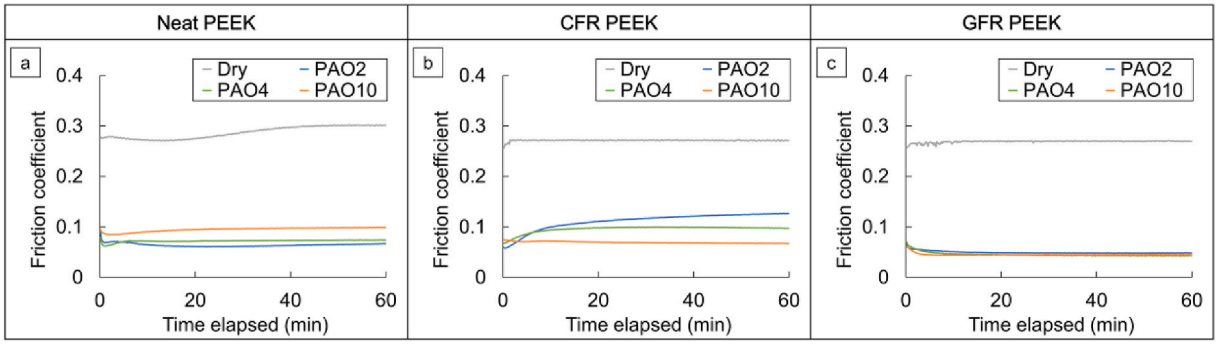

Fig. 2. Friction coefficients as a function of time (a) neat PEEK, (b) CFR PEEK and (c) GFR PEEK.

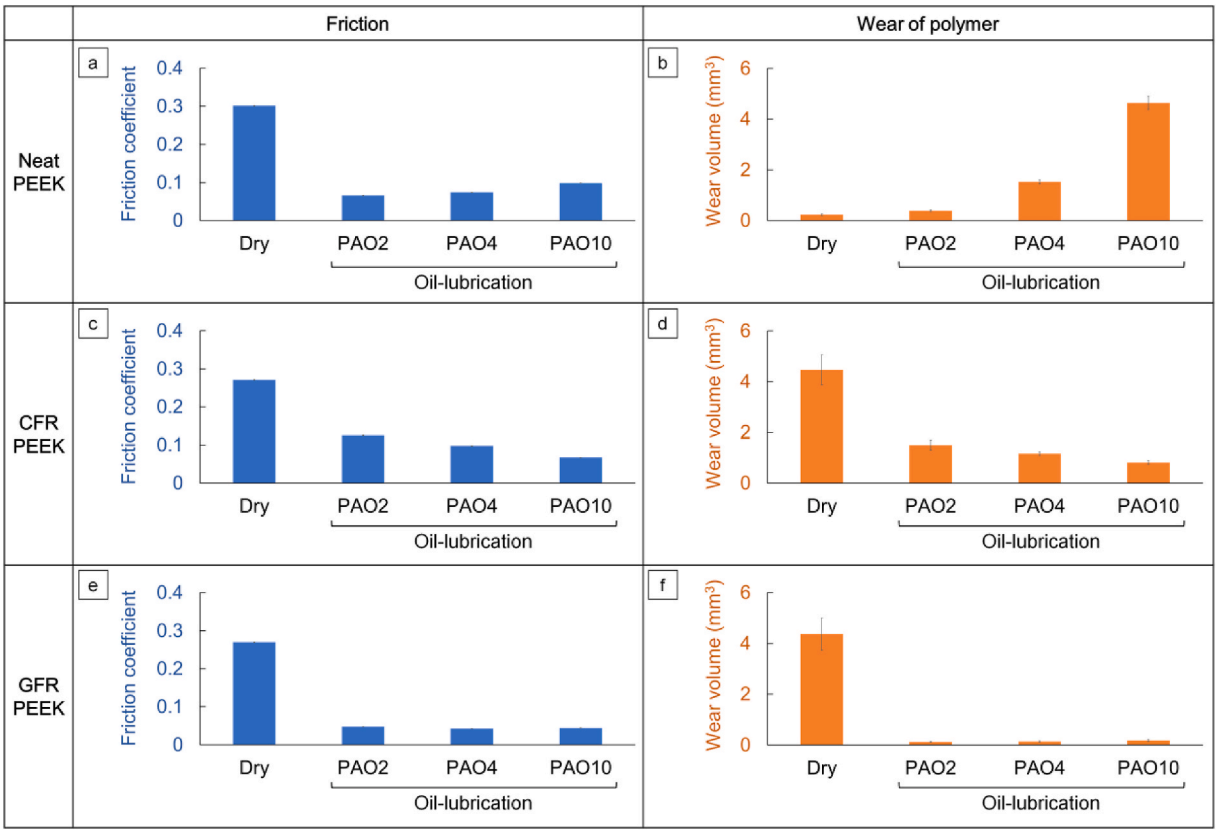

Fig. 3. Friction coefficients averaged during the last 10 min and wear volumes of polymer plates (a, b) neat PEEK, (c, d) CFR PEEK and (e, f) GFR PEEK. Error bars designate ± one standard deviation.

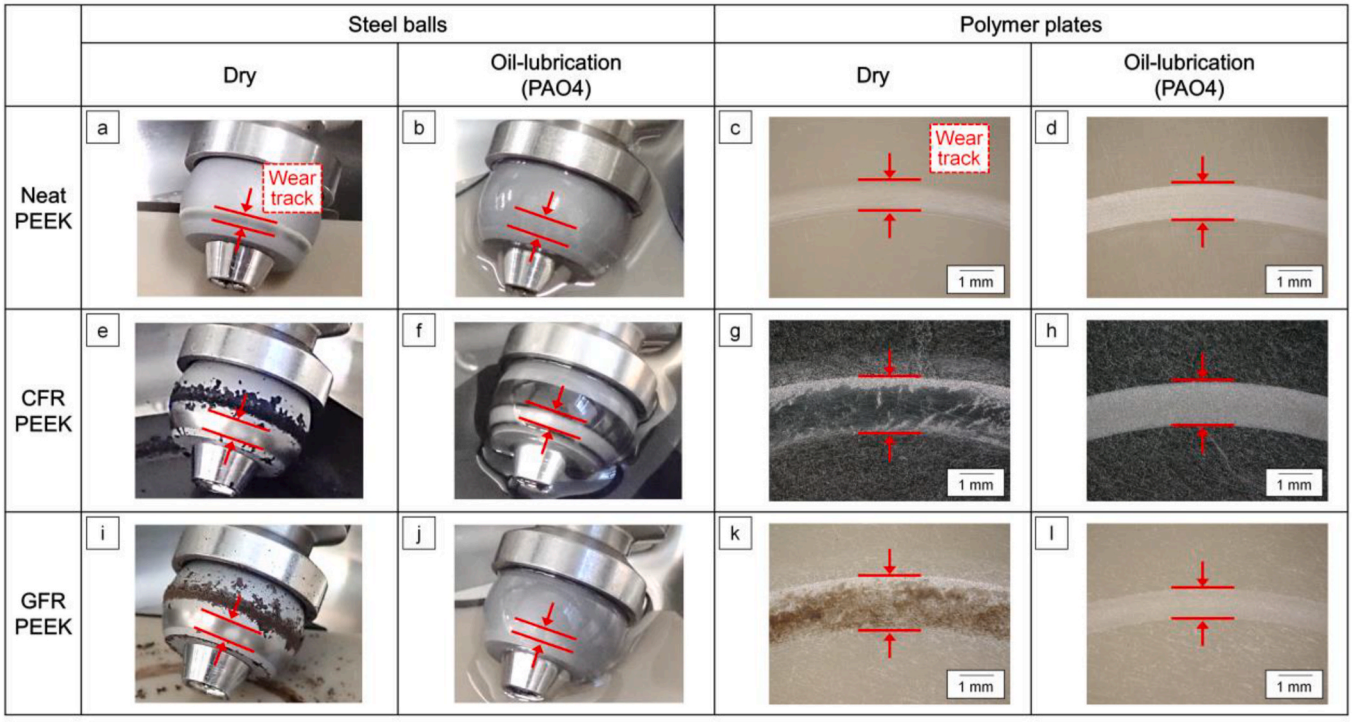

Fig. 4. Appearance of steel balls and polymer plates tested under dry conditions and lubrication with PAO4 (a–d) neat PEEK, (e–h) CFR PEEK and (i–l) GFR PEEK.

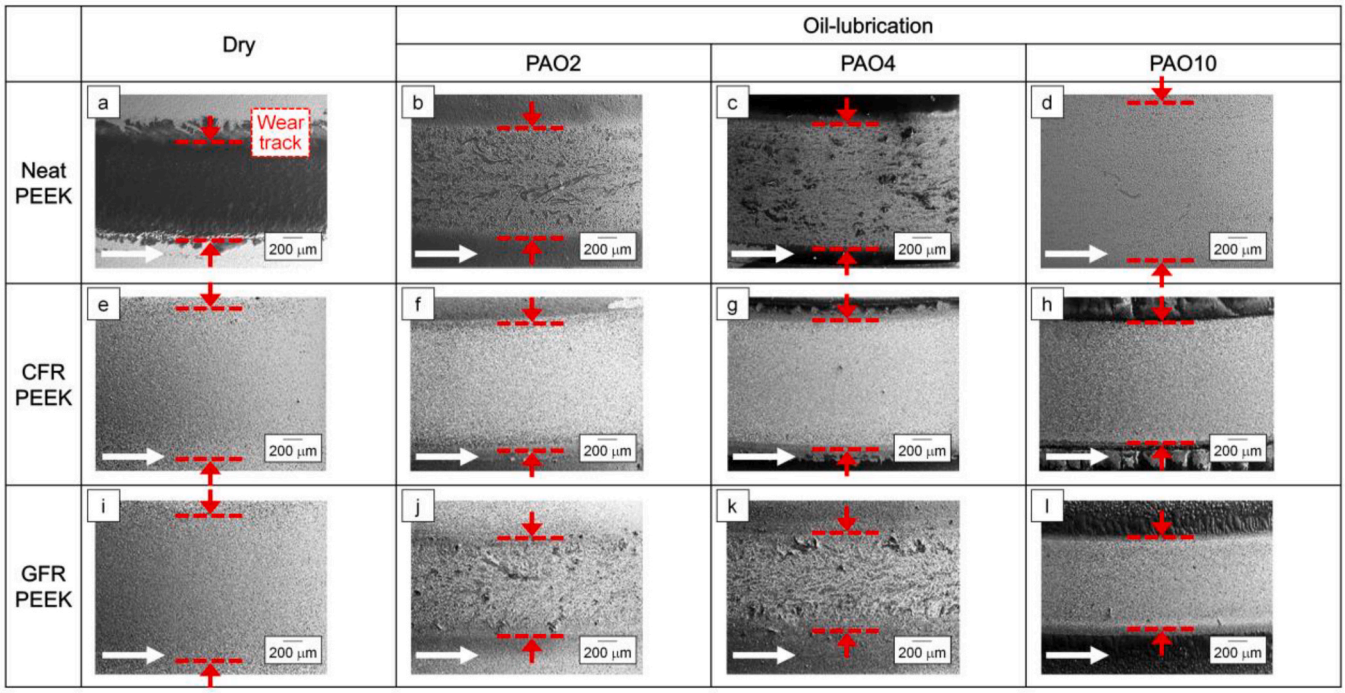

Fig. 5. SE images of steel balls tested under dry conditions and lubrication with PAO2, PAO4 and PAO10 (a–d) neat PEEK, (e–h) CFR PEEK and (i–l) GFR PEEK. Arrows indicate the sliding direction.

films were formed by neat PEEK and GFR PEEK (Fig. 5(b, c, j, k)). CFR PEEK did not form any transfer films regardless of the PAO viscosity grade used (Fig. 5(f–h)). Although SE images show that there are differences between the polymer transfer films, EPMA carbon mapping was required to evaluate the film, specifically the amount of polymer of each transfer film (Fig. 6(a–l)). The amount of carbon in the transfer film is indicated by the color scale on the map. For each polymer material, a good correlation can be seen between the carbon amount transferred on the wear track of steel balls (Fig. 6(a–l)) and the wear volumes of polymer plates (Fig. 3(b, d, f)) e.g. larger amounts of carbon detected on the wear tracks of steel balls were conducive to lower wear volumes of polymer plates. This emphasizes the importance of the transfer film in reducing polymer wear. As previously shown [34], the carbon detected with EPMA originates from PEEK, which in this study originates from the neat PEEK or the PEEK matrix in GFR PEEK plates. Although the EPMA measured carbon can be derived from the carbon fibers in CFR

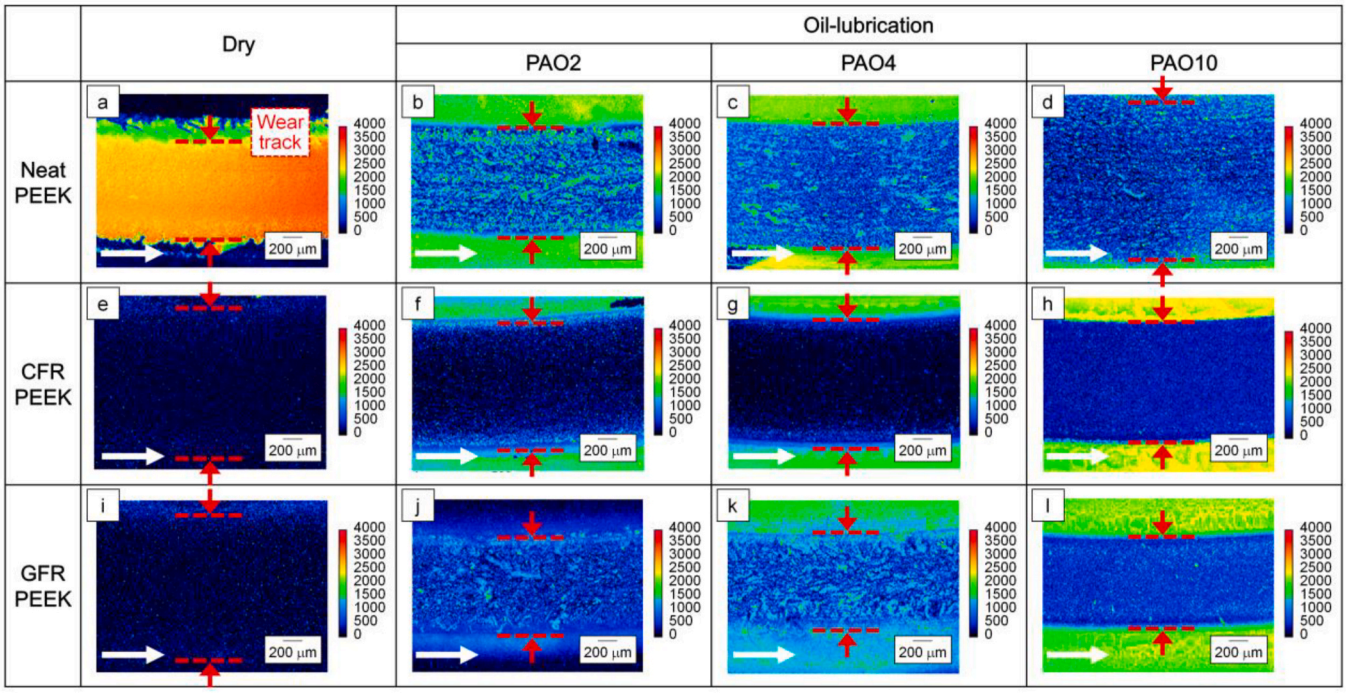

Fig. 6. EPMA carbon maps of steel balls tested under dry conditions and lubrication with PAO2, PAO4 and PAO10 (a–d) neat PEEK, (e–h) CFR PEEK and (i–l) GFR PEEK. Arrows indicate the sliding direction.

PEEK, in these analyses no carbon was detected on the wear tracks which simplifies the interpretation. The balls paired with neat PEEK and GFR PEEK lubricated with PAO4 showed almost the same amount of carbon on their wear tracks (Fig. 6(c, k)), while the wear of the GFR PEEK plate was lower than that of neat PEEK (Fig. 3(b, f)). This is explained by the superior mechanical strength of GFR PEEK than that of neat PEEK. The friction coefficients of lubricated neat PEEK tests and GFR PEEK tests became stable shortly after starting the tests (Fig. 2(a, c)), implying that their polymer transfer films were formed immediately in the running in process. Note that under PAO10 lubricated conditions which generated less polymer transfer films for all polymers (Fig. 6(d, h, l)), neat PEEK gave much higher wear volumes than CFR PEEK and GFR PEEK (Fig. 3(b, d, f)), thus the wear results here reflect their mechanical strength.

In terms of comparison with the dry conditions, while oil-lubrication inhibited the formation of polymer transfer films for neat PEEK, it accelerated it for GFR PEEK. CFR PEEK did not perform differently under dry or oil-lubrication. Further investigation was necessary to understand the effect of oil-lubrication on the formation of polymer transfer films, though the tribological properties under oil-lubrication were clearly related to the amount of the polymer transfer films on the steel counterparts. Because the reinforcement fibers in PEEK composites are much harder than the matrix, the formation of polymer transfer films on the steel counterparts will be influenced by the fibers present on the polymer surfaces. Therefore, surface analysis of polymer plates was conducted and is reported in sections 3.3 and 3.4.

3.3. Optical 3D measurements of polymer plates

The wear tracks of polymer plates were investigated with Alicona optical profilometry. Fig. 7(a–l) and Fig. 8(a–l) show the optical images and the corresponding 3D surface profiles of the wear tracks on polymer plates. The dry and oil-lubricated polymer material looked totally different in each case. The neat PEEK wear track under dry condition was relatively smooth and shows lines in the sliding direction with small marks which is characteristic of adhesive wear (Figs. 7(a), Fig. 8(a)). Under oil-lubrication characteristic features of abrasion were shown (Fig. 7(b–d), Fig. 8(b–d)), as observed by Schallamach [51] for the abrasive wear of rubber. This became more obvious under lubrication with the higher viscosity PAO, indicating that under oil-lubrication, abrasion was the dominating mechanism responsible for the high wear of neat PEEK.

The CFR and GFR PEEK tested under dry conditions produced similar wear tracks showing piled up wear debris containing fractured fibers (Fig. 7(e, i), Fig. 8(e, i)). These results support the hypothesis that three-body abrasion by wear debris containing hard reinforcement fibers caused the large wear of CFR and GFR PEEK plates under dry conditions. However, as the oil-lubrication flushed wear debris out from the contact surfaces, the wear tracks then had a smooth appearance as shown in Fig. 8(f-h, j-l). CFR PEEK and GFR PEEK contain the same weight percentage of carbon fibers and glass fibers, respectively, but the volume percentage is about 1.4 times higher for carbon fibers in CFR PEEK than that of glass fibers in GFR PEEK due to the difference in the specific weights of carbon fiber (approximately 1.8) and glass fiber (approximately 2.5). Interestingly, as shown in Fig. 7(f-h, j-l) the amount of fibers observed on the wear tracks of CFR PEEK under oil-lubrication was much larger than that of GFR PEEK, even after taking into account the difference in fiber volume percentages.

In addition, on the wear tracks of CFR PEEK, finely fractured fibers (with sizes less than 20 μm) compared to the 100–200 μm present in new plates were observed and detected in larger amounts under lubrication with lower viscosity PAOs (Fig. 7(f–h)). Furthermore, these fractured carbon fibers became exposed from the PEEK matrix (Fig. 8(f–h)). As fractured fibers are expected to be produced continuously during testing, and thus their amount increases as the test progresses, the friction coefficients in the CFR PEEK tests lubricated with PAO2 and PAO4 would be expected to increase with time as was found in Fig. 2(b). On the other hand, the glass fibers observed on the wear tracks of GFR PEEK under oil-lubrication appeared less damaged and PAO2, PAO4 and PAO10 provided similar wear track appearances (Fig. 7(j–l)). Additionally, in Fig. 7(j–l) and Fig. 8(j–l) the glass fibers seemed to be well embedded in the grooves. This was also confirmed by nanoindentation hardness mapping in section 3.4.

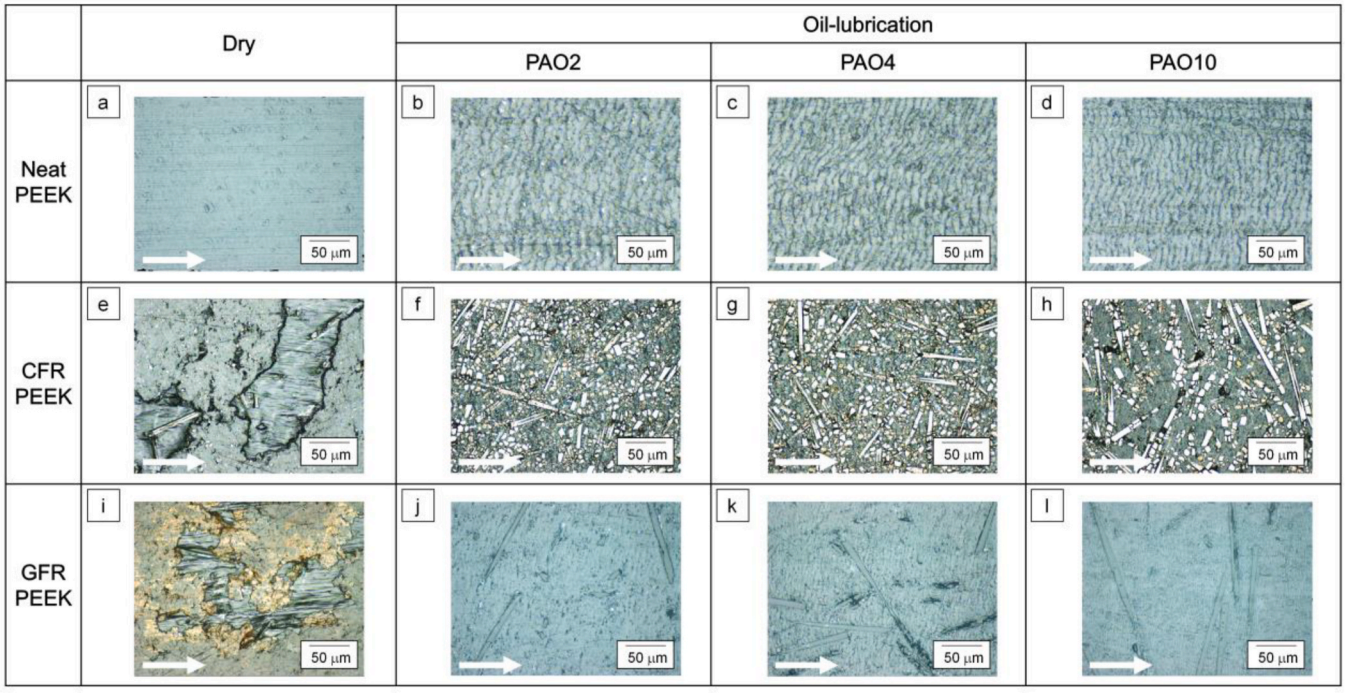

Fig. 7. Optical images of wear tracks on polymer plates tested under dry conditions and lubrication with PAO2, PAO4 and PAO10 (a–d) neat PEEK, (e–h) CFR PEEK and (i–l) GFR PEEK. Arrows indicate the sliding direction.

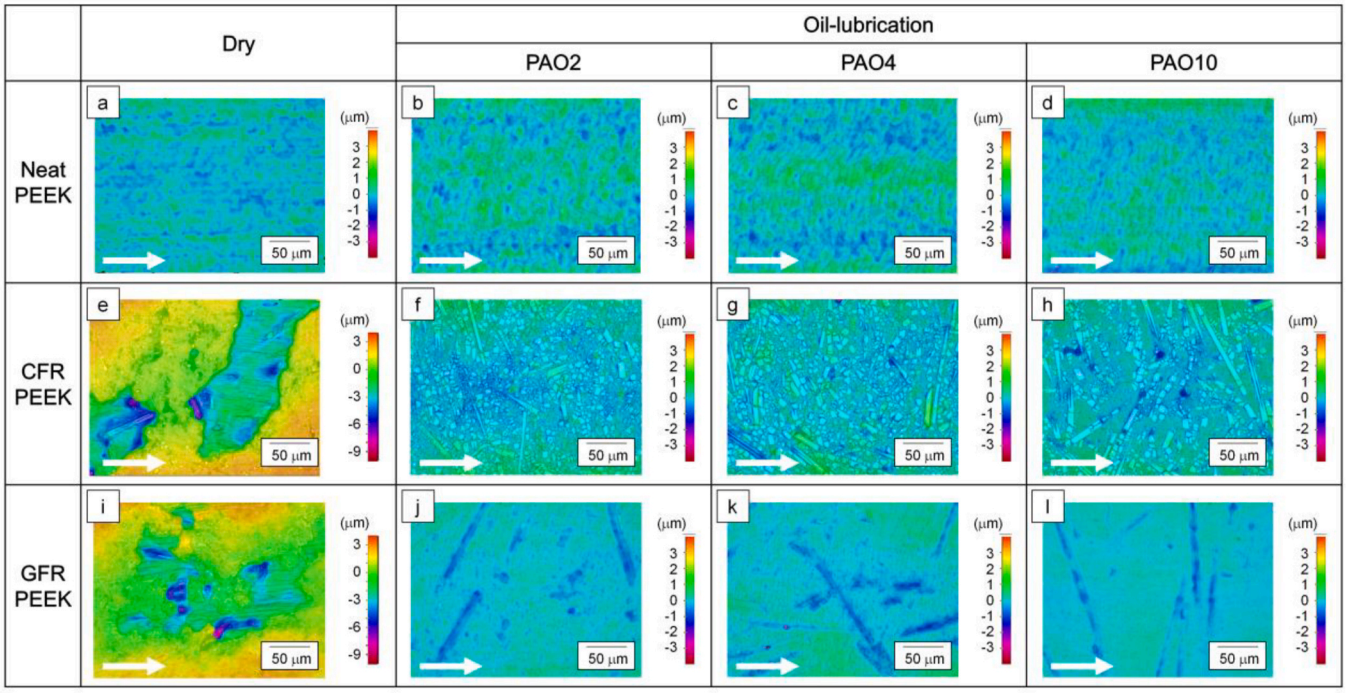

Fig. 8. 3D surface profiles of wear tracks on polymer plates tested under dry conditions and lubrication with PAO2, PAO4 and PAO10 (a–d) neat PEEK, (e–h) CFR PEEK and (i–l) GFR PEEK. Arrows indicate the sliding direction.

3.4. Nanoindentation measurements of polymer plates

Continuous stiffness measurement and hardness mapping of polymer surfaces were carried out as described in section 2.3. The continuous stiffness measurement technique was initially employed to evaluate the wear tracks of neat PEEK plates from dry and oil-lubricated tests. The hardness values were plotted as a function of indentation depth and compared to those of a new PEEK plate (Fig. 9(a–d)). In all tests, high values of hardness were measured at indentation depth <0.5 μm. These values are thought to be attributed to a phenomenon known as the indentation size effect (ISE), and are not regarded as physically significant because they are distorted by the inadequacies in the procedures applied to provide corrections for the imperfections in the tip geometry [49,52]. Therefore, only hardness values at indentation depth >0.5 μm were taken into account in the following discussions.

The wear track from the dry condition testing showed almost the same hardness values as the new plate (Fig. 9(a)), while the wear tracks from oil-lubrication were softened regardless of the PAO viscosity grades used (Fig. 9(b–d)). The PEEK softening in the PAO2, PAO4 and PAO10 tests was similar and contrasts with the large differences in their friction and wear performances which depended on the viscosity of PAO (Fig. 3 (a and b)). As mentioned in previous studies [53,54], assuming that the hardness modification is related to the permeation of fluid molecules into polymer surfaces, the molecular sizes of all viscosity grades of PAO used in this study are plausibly small enough to permeate the surface. Nevertheless, the continuous stiffness measurement results indicate there was no correlation between the hardness of polymer surfaces and the tribological properties of neat PEEK.

Secondly, hardness mapping measurements were carried out on the wear tracks of polymer plates lubricated with PAO4. As shown in section 3.3, the wear tracks lubricated with PAO2, PAO4 and PAO10 looked similar for each polymer material. Hardness mapping measurements were used to investigate the distribution of reinforcement fibers on the polymer surfaces and in this respect the wear tracks lubricated with PAO4 were considered representative and compared with the new plates. Fig. 10(a–l) show the optical images of the polymer plates and their corresponding hardness maps where the color scale indicates the hardness values. The small indents were observed over the entire surface of the optical images, because these images were acquired after indentation.

For each polymer material, the hardness map of the new plates showed a uniform hardness with values below 0.5 GPa for most parts.

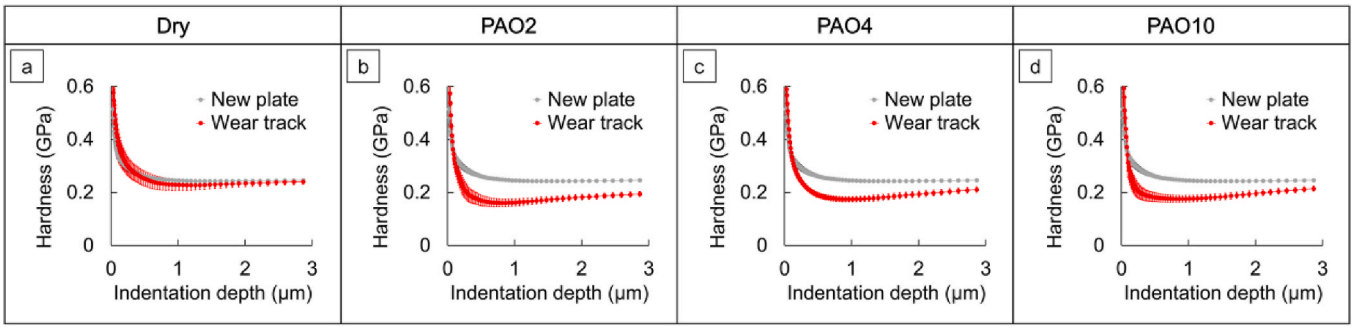

Fig. 9. Nanoindentation hardness of wear tracks on neat PEEK polymer plates tested under (a) dry conditions, and lubrication with (b) PAO2, (c) PAO4 and (d) PAO10. Error bars designate ± one standard deviation.

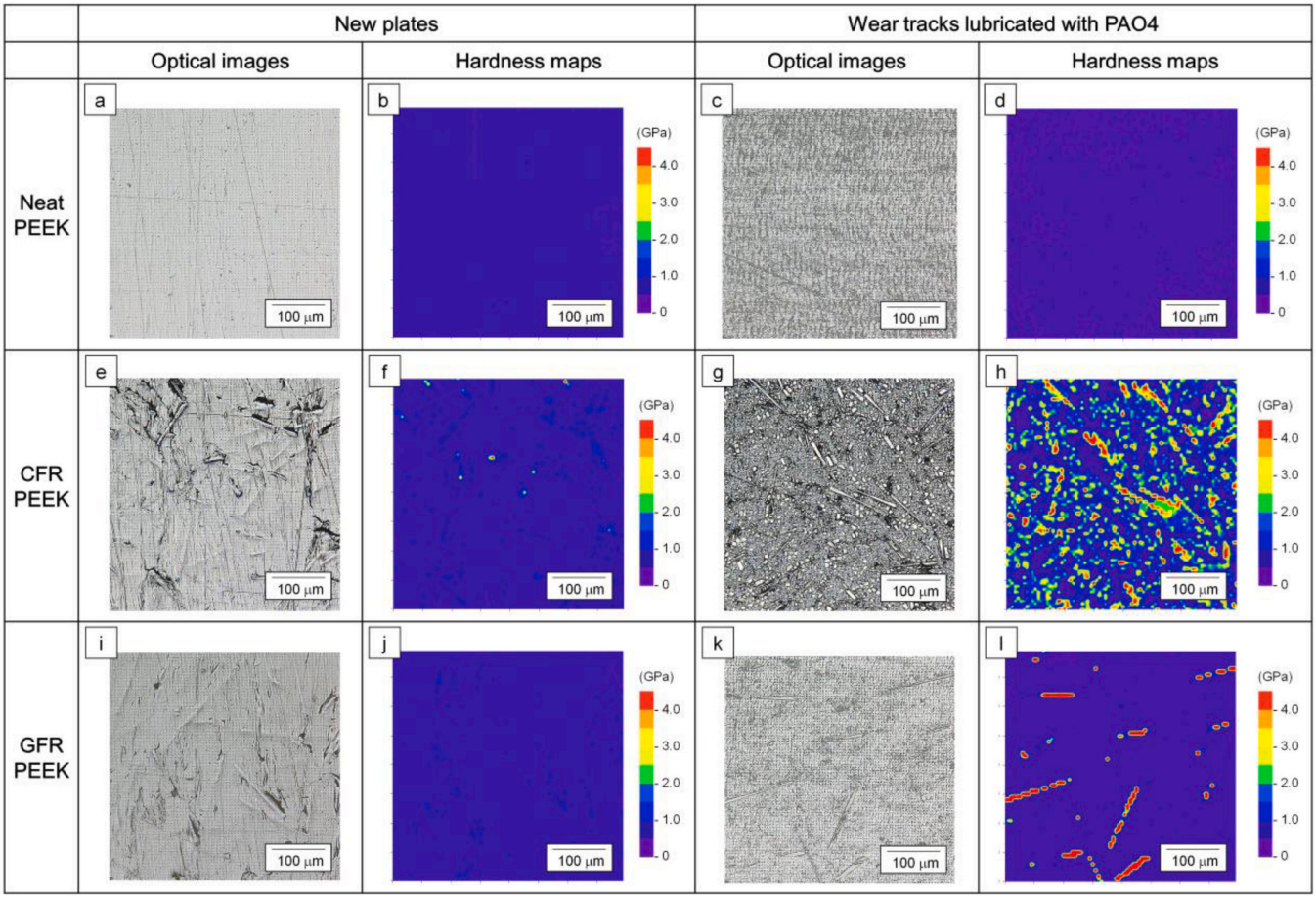

Fig. 10. Optical images and nanoindentation hardness maps of new plates and wear tracks on polymer plates lubricated with PAO4 (a–d) neat PEEK, (e–h) CFR PEEK and (i–l) GFR PEEK.

This indicates that the reinforcement fibers were not exposed from the PEEK matrix, except for small areas of the CFR PEEK surface (Fig. 10(f)). The wear track of neat PEEK lubricated with PAO4 showed a uniform hardness map (Fig. 10(d)), but the hardness values and results from the continuous stiffness measurement (Fig. 9(c)) were slightly lower than for the new plate. Numerous areas of high hardness (values over 1.0 GPa) were detected on the wear tracks of CFR and GFR PEEK lubricated with PAO4 (Fig. 10(h, l)). These areas matched well the distributions of the exposed fibers observed in the corresponding optical images (Fig. 10 (g, k)). As discussed in section 3.3, fractured fibers were observed to be densely distributed on the wear tracks of oil-lubricated CFR PEEK (with sizes less than 20 μm compared to the 100–200 μm in new plates). The hardness map in Fig. 10(h) confirmed that these more or less damaged fibers contributed to the hardness values of the wear tracks. Although the hardness mapping measurements were only carried out for the wear tracks lubricated with PAO4, the results for the wear tracks lubricated with PAO2 and PAO10 are expected to show the same trend based on the fiber distributions observed in the optical images (Fig. 7(f, h)). The PEEK matrix of the PAO4 lubricated wear track of CFR and GFR PEEK had almost the same hardness as the PAO4 lubricated neat PEEK wear track. This implies that the hardness of polymer surfaces in the CFR and GFR PEEK tests could be influenced by the exposed reinforcement fibers even when lubricated with different viscosities PAOs.

The results from this section and section 3.3 suggest that the reinforcement fibers exposed on the wear tracks of polymer plates played an important role in tribological properties under oil-lubrication, especially for CFR and GFR PEEK. However, the mechanism of action still remains unclear: what is the influence of the wear debris under oil-lubrication? As mentioned in section 3.3, wear debris of CFR and GFR PEEK containing hard reinforcement fibers caused the large wear of polymer plates under dry conditions. Although the wear debris was flushed out from the contact surfaces by the oil, it still remained dispersed in the oils and possibly influencing the tribological performances directly and/or indirectly. Therefore, an additional test was devised to investigate the influence of wear debris.

3.5. *Lubrication with PAO4 containing CFR PEEK wear debris*

An additional test was performed on GFR PEEK lubricated with the PAO4 oil containing CFR PEEK wear debris. The test oil was prepared by collecting the PAO4 oil previously used in a CFR PEEK test which thus contained dispersed CFR PEEK wear debris with the sizes up to 20 μm. Fig. 11(a) shows the friction coefficient values as a function of time for this test in comparison with CFR and GFR PEEK lubricated with pristine PAO4. The wear-debris-containing PAO4 gave slightly higher friction than PAO4 lubricated GFR PEEK, but much lower friction than PAO4 lubricated CFR PEEK. A similar trend was observed for the wear of polymer plates (Fig. 11(b)): the wear-debris-containing PAO4 slightly increased the wear of GFR PEEK plate compared to pristine PAO4, but the wear was still distinctively lower than that of CFR PEEK lubricated with pristine PAO4. Similar results have been reported by Kunishima et al. [55] who studied the effect of glass fibers wear debris contained in lubricant grease on the tribological properties of GFR polyamide 66 paired with steel counterparts. They concluded that the wear debris contained in the grease did not affect the friction and wear of the polymer composite.

Fig. 12(a and b) shows the polymer transfer film on the steel ball wear track analyzed with EPMA as discussed in section 3.2. (Figs. 5(k),

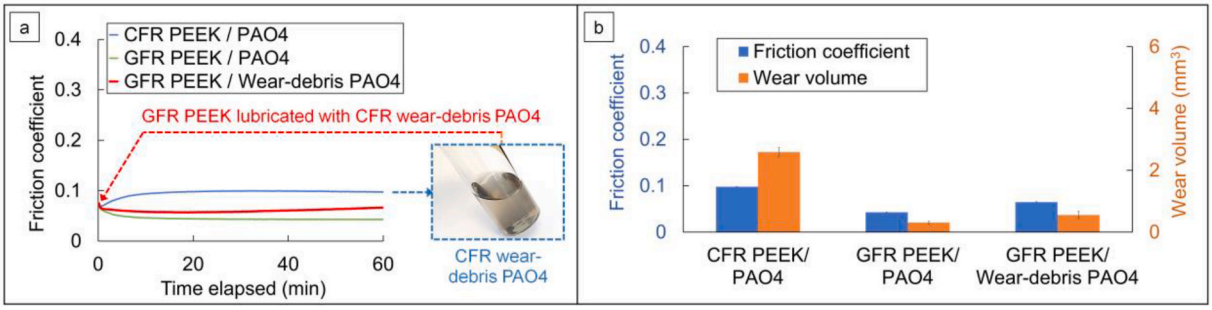

Fig. 11. (a) Friction coefficients as a function of time, and (b) friction coefficients averaged during the last 10 min and wear volumes of polymer plates. Error bars designate ± one standard deviation.

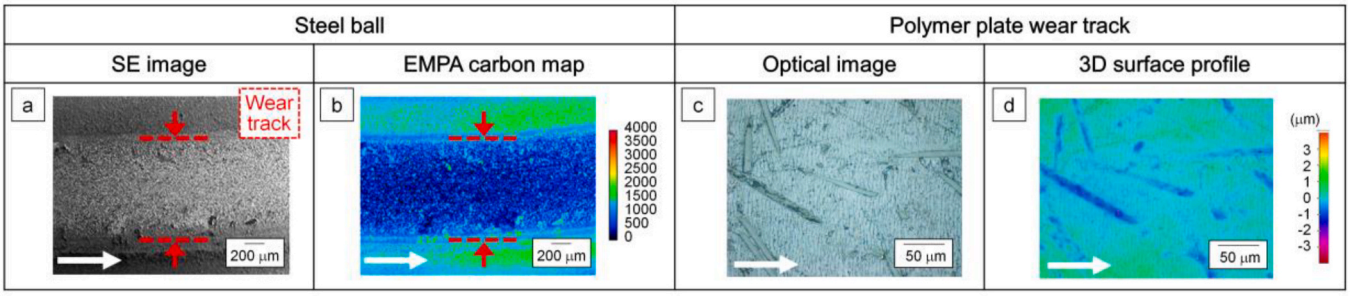

Fig. 12. (a) SE image and (b) EPMA carbon map of steel ball, and (c) optical image and (d) 3D surface profile of wear track on polymer plate in GFR PEEK test lubricated with PAO4 containing CFR PEEK wear debris. Arrows indicate the sliding direction.

Fig. 6(k)). The wear-debris-containing PAO4 led to less transfer film than pristine PAO4 in GFR PEEK tests. This indicates CFR PEEK wear debris inhibited the formation of the polymer transfer film. However, PAO4 lubricated CFR PEEK generated an even thinner transfer film. GFR PEEK lubricated with wear-debris-containing PAO4 gave an almost similar optical image and 3D surface profile to pristine PAO4 while fractured carbon fibers were hardly observed on the wear track (Figs. 7(k), 8(k) and 12(c and d)). This implies that the fractured carbon fibers formed on the CFR PEEK wear tracks (Fig. 7(f, g, h)) once flushed out from the polymer surfaces by the oils as wear debris, would not stick again.

These results show that the wear debris containing hard reinforcement fibers is harmful to friction and wear but not as much as the exposed fibers on the wear tracks of polymer plates as discussed in section 3.4. This and the polymer transfer film results in section 3.2, have enabled us to develop a clearer picture of the situation and propose a mechanism of action, discussed in section 3.6.

3.6. Mechanism of oil-lubrication

To understand the mechanism of oil-lubrication, the Lambda ratios represented as the oil film thicknesses to the composite roughness of two contact surfaces (polymer and steel) were calculated for each condition and are included in Table 3. The Lambda value for non-fluid lubricated tests (dry conditions) is zero for all polymers. Fig. 13(a and b) summarizes the averaged friction coefficients during the last 10 min of testing and the wear volumes of the polymer plates as a function of the Lambda ratios. The oil film thicknesses were estimated from the equations for piezoviscous-elastic lubrication [56]. Note that the test conditions employed in this study were borderline between piezoviscous-elastic and isoviscous-elastic lubrication, however, the oil film thickness calculations using the equations for piezoviscous-elastic and isoviscous-elastic lubrication [57,58] gave almost the same results. Based on the calculated values of Lambda ratios being less than one for all test conditions, the tribological testing in this study was considered to be performed in the boundary lubrication regime. Theoretically, the higher Lambda ratios lead to lower friction and wear and this trend is observed for CFR PEEK lubricated with PAOs of increasing viscosity and therefore increasing Lambda values. Unexpectedly, the trends for the neat PEEK and GFR PEEK tests did not follow this trend. In the neat PEEK tests the higher Lambda ratios resulted in higher friction coefficients and wear volumes of the polymer plates, while for GFR PEEK tests there was no dependence of the tribological results on the Lambda ratios. However, the different responses of the polymer materials to the Lambda ratios correlate well with the amount of the polymer transfer films on the steel balls. The neat PEEK and GFR PEEK tests at lower Lambda ratios formed thick polymer transfer films which through their protective role prevent friction and wear (Fig. 5(b, c, j, k)). As a result, their friction and wear were lower than might be expected from the Lambda ratios. Lower Lambda ratios led to thicker transfer films for both the neat PEEK and GFR PEEK. On the other hand, under dry conditions a different trend was observed; the neat PEEK formed the thickest transfer film while GFR

Table 3
Test conditions and calculated Lambda ratios.

Material paring		Entrainment speed	Applied load	Temperature	Lambda ratios		
Plate	Ball	(m/s)	(N)	(°C)	PAO2	PAO4	PAO10
Neat PEEK	Steel	0.5	50	25	0.05	0.15	0.45
CFR PEEK	Steel	0.5	50	25	0.04	0.11	0.34
GFR PEEK	Steel	0.5	50	25	0.04	0.12	0.37

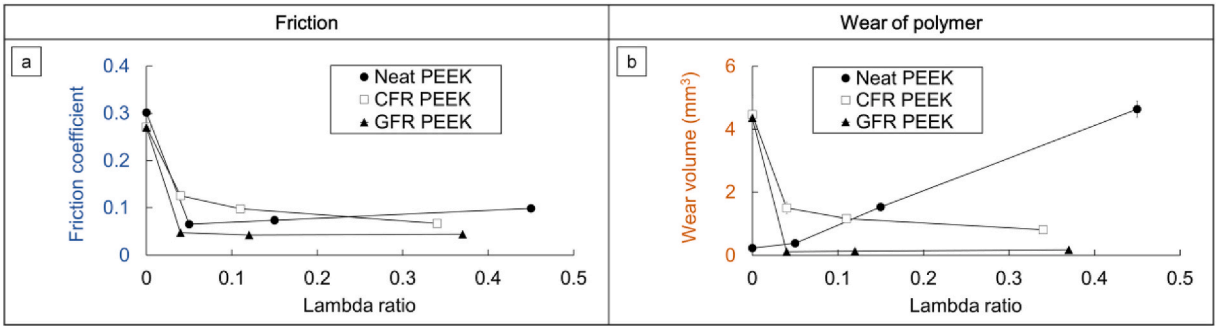

Fig. 13. (a) Friction coefficients averaged during the last 10 min and (b) wear volumes of polymer plates as a function of Lambda ratios.

PEEK provided almost no film.

We have reported previously [34] that oil-lubrication suppressed not only the formation but also the removal of polymer transfer films in the PEEK-steel contact, and their balance depends on the tribological test conditions. The Lambda ratio investigated in this study is another important factor which may affect this balance and the proposed mechanism of action is summarized in Fig. 14. Note that although the two contact surfaces of the steel ball and polymer plate are drawn as slightly separated in all schematics, due to Lambda ratios being less than one, they are actually in partial contact under oil-lubrication.

When comparing the tribological performance in dry and oil-lubrication, wear debris is found to play a key role. In the neat PEEK tests under dry condition, wear debris contributed to the formation of polymer transfer films and thus provides thick films. Oil-lubrication flushes out wear debris from the contact surfaces, increasing friction and wear in the neat PEEK tests. On the other hand, in the CFR and GFR PEEK tests, wear debris, which contain hard reinforcement fibers, causes three-body abrasion under dry conditions. In this case, oil-lubrication flushed out wear debris from the contact surfaces and reduced friction and wear. As the wear debris up to 20 μm in size was larger than the oil film thicknesses (approximately 0.2 μm with the more viscous oil PAO10), the wear debris once dispersed into the PAO oils is less likely to re-enter the contact surfaces, especially so for the ball-on-disc configuration adopted in this study where the debris is expected to flow mainly outside the contact area. This explains why the PAO4 oil containing the CFR PEEK wear debris gave similar result to the new PAO4, as investigated in section 3.5.

The differences in tribological performance between neat PEEK, CFR PEEK and GFR PEEK tests under oil-lubrication is explained by two important factors, the polymer transfer films on steel counterparts and the hardness modification of the polymer surfaces. These factors are also related to each other, as seen in the CFR and GFR PEEK tests. When neat PEEK is oil lubricated, the formation of polymer transfer films is inhibited and this negative effect becomes more prominent as the viscosity of PAO increases. On the other hand, in the CFR PEEK tests, the fractured carbon fibers exposed on the polymer surface wear off by abrasion the polymer transfer films on steel counterparts and thus inhibit film formation even more strongly than oil-lubrication. In addition, as pointed by Chen et al. [32], the fractured carbon fibers may decrease the load carrying capacity, further increasing friction and wear. Notably, compared to these exposed fibers, wear debris flushed out from the contact surfaces seems to be less influential on friction and wear, even though it is carried around/circulated in the oil. In the GFR PEEK tests, oil-lubrication inhibits the formation of polymer transfer film as in the case of neat PEEK. However, due to the superior mechanical strength of GFR PEEK, its friction and wear performance is far superior to that of neat PEEK. Remarkably, the glass fibers on the wear tracks were less damaged and better embedded in the PEEK matrix, therefore not causing the negative effect seen in the case of exposed carbon fibers.

Apart from the type of reinforcement fibers, several other factors have been reported to influence the tribological properties of PEEK and its composites under dry conditions, such as the polymer production process, fiber contents, and fiber orientations [8,59,60]. These factors could also affect the tribological properties under oil-lubrication. Nevertheless, this study brings novel insight into the effect of oil-lubrication on the tribological properties of PEEK and its composites by elucidating the mechanism of action. This knowledge is essential to formulating optimal lubricants and developing more efficient systems for PEEK applications.

4. Conclusions

The effect of oil-lubrication on the tribological properties of neat PEEK, CFR PEEK and GFR PEEK paired with steel counterparts has been investigated by using various viscosity grades of PAO. The results were analyzed by focusing on two key factors, the polymer transfer films on the steel counterparts and the hardness modification of the polymer surfaces, with the aim of revealing the mechanism of action. The following conclusions have been drawn:

(1) Compared to the dry conditions, oil-lubrication reduced friction regardless of the type of polymer materials. The wear behavior

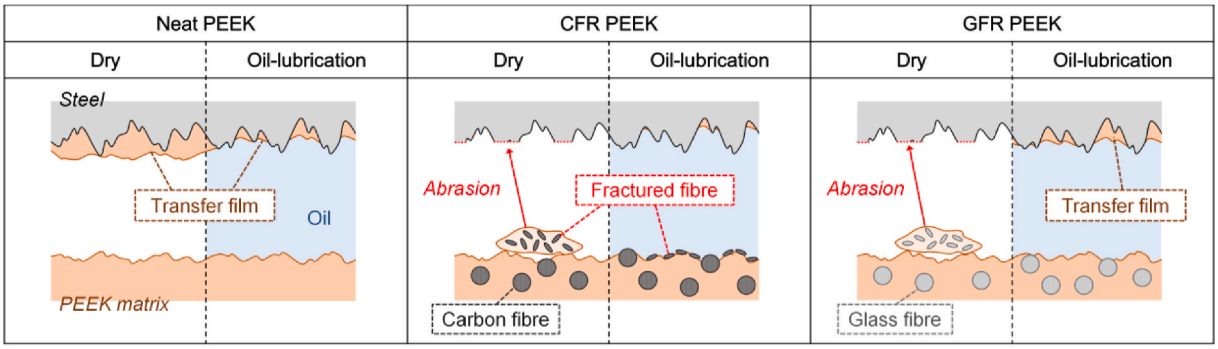

Fig. 14. Proposed mechanism of oil-lubrication of neat PEEK, CFR PEEK and GFR PEEK paired with steel counterparts.

depended on the polymer type, it increased for neat PEEK and decreased for CFR and GFR PEEK;

(2) The higher viscosity grades of PAO led to higher friction and wear of polymers for neat PEEK. By contrast, the CFR PEEK performed better when lubricated with higher viscosity PAOs. The GFR PEEK performance was less influenced by the PAO viscosity and showed the lowest friction and wear under oil-lubrication;

(3) The amount of polymer transfer films formed on steel counterparts, as measured by EPMA carbon maps, correlated well with the tribological properties. Thick films were observed for neat PEEK and GFR PEEK even under oil-lubrication (PAO2 and PAO4). In contrast, CFR PEEK did not form transfer films in either dry or oil-lubrication conditions;

(4) The wear tracks on neat PEEK plates were softened under oil-lubrication, regardless of the oil viscosity grades used which indicates that polymer softening did not dominate the tribological properties in this study;

(5) Numerous fractured fibers were exposed on the wear tracks of CFR PEEK plates after testing, possibly inhibiting the formation of polymer transfer films on steel counterparts. By contrast, the wear tracks on GFR PEEK plates showed well matrix embedded and less damaged fibers, enabling the formation of transfer films similar to those found on neat PEEK.

This study has elucidated the effect of oil-lubrication of PEEK and its composites when paired with steel counterparts and has informed on its mechanism of action. This knowledge contributes to the design of efficient tribological systems and the formulation of suitable lubricants for PEEK applications, thus promoting the adoption of green technologies in many engineering applications.

Funding

This work was supported by ENEOS Corporation, Japan.

Declaration of competing interest

The authors declare that they have no known competing financial interests or personal relationships that could have appeared to influence the work reported in this paper.

Acknowledgements

The authors would like to thank the Analytical Technology group from R&D Solution Center, ENEOS Corporation for performing the EPMA.

References

[1] N.K. Myshkin, S.S. Pesetskii, A.Y. Grigoriev, Tribol. Ind. 37 (2015) 284.
[2] R. Gandhi, A. Jayawant, A. Bhalerao, R. Dandagwhal, Int. J. Eng. Sci. Invent. 7 (2018) 36.
[3] K. Friedrich, Adv. Ind. Eng. Polym. Res. 1 (2018) 3.
[4] A. Kurdi, L. Chang, Lubricants 7 (2018) 2.
[5] L. Zhang, Y. Sawae, T. Murakami, H. Yang, K. Yuki, Tribol. Online 10 (2015) 404.
[6] M. Regis, A. Lanzutti, P. Bracco, L. Fedrizzi, Wear 408–409 (2018) 86.
[7] A. Schelling, H.H. Kausch, A.C. Roulin, Wear 151 (1991) 129.
[8] Z.P. Lu, K. Friedrich, Wear 181–183 (1995) 624.
[9] K.A. Laux, C.J. Schwartz, Wear 301 (2013) 727.
[10] T.J. Hoskins, K.D. Dearn, Y.K. Chen, S.N. Kukureka, Wear 309 (2014) 35.
[11] K.A. Laux, A. Jean-Fulcrand, H.J. Sue, T. Bremner, J.S.S. Wong, Polymer 103 (2016) 397.
[12] M. Zalaznik, M. Kalin, S. Novak, Tribol. Int. 94 (2016) 92.
[13] L. Lin, X.Q. Pei, R. Bennewitz, A.K. Schlarb, Tribol. Int. 122 (2018) 108.
[14] M. Yahiaoui, F. Chabert, J.Y. Paris, V. Nassiet, J. Denape, *Tribol. Int.* 132 (2019) 154.
[15] D. Walton, Y.W. Shi, Proc. Inst. Mech. Eng. Part C J. Mech. Eng. Sci. 203 (1989) 31.
[16] C.J. Hooke, S.N. Kukureka, P. Liao, M. Rao, Y.K. Chen, Wear 200 (1996) 83.
[17] B.J. Briscoe, S.K. Sinha, Proc. Inst. Mech. Eng. Part J J. Eng. Tribol. 216 (2002) 401.
[18] A.K. Singh, Siddhartha, P.K. Singh, Proc. Inst. Mech. Eng. Part J J. Eng. Tribol. 232 (2018) 210.
[19] M. Harrass, K. Friedrich, A.A. Almajid, Tribol. Int. 43 (2010) 635.
[20] A. Kurdi, W.H. Kan, L. Chang, Tribol. Int. 130 (2019) 94.
[21] R. Schroeder, F.W. Torres, C. Binder, A.N. Klein, J.D.B. De Mello, Wear 301 (2013) 717.
[22] D. Kumar, T. Rajmohan, S. Venkatachalapathi, Mater. Today Proc. 5 (2018) 14583.
[23] W. Qihua, X. Jinfen, S. Weichang, L. Weimin, Wear 196 (1996) 82.
[24] I. Minami, T. Kubo, H. Nanao, S. Mori, H. Iwata, M. Fujita, Tribol. Online 3 (2008) 190.
[25] A.C. Greco, R. Erck, O. Ajayi, G. Fenske, Wear 271 (2011) 2222.
[26] M. Kalin, M. Zalaznik, S. Novak, Wear 332–333 (2015) 855.
[27] V. Rodriguez, J. Sukumaran, A.K. Schlarb, P. De Baets, Tribol. Int. 103 (2016) 45.
[28] G. Theiler, T. Gradt, Wear 368–369 (2016) 278.
[29] L. Lin, A.K. Schlarb, Tribol. Int. 137 (2019) 173.
[30] J. Jia, J. Chen, H. Zhou, L. Hu, Tribol. Lett. 17 (2004) 231.
[31] M. Sumer, H. Unal, A. Mimaroglu, Wear 265 (2008) 1061.
[32] B. Chen, J. Wang, F. Yan, Tribol. Int. 52 (2012) 170.
[33] G. Zhang, B. Wetzel, Q. Wang, Tribol. Int. 88 (2015) 153.
[34] G. Tatsumi, M. Ratoi, Y. Shitara, K. Sakamoto, B.G. Mellor, Tribol. Online 14 (2019) 345.
[35] T.F. de Andrade, H. Wiebeck, A. Sinatora, Polimeros 29 (2019) 3.
[36] C. Wu, C. Wei, X. Jin, R. Akhtar, W. Zhang, J. Mater. Sci. 54 (2019) 5127.
[37] G. Yu, H. Liu, K. Mao, C. Zhu, P. Wei, Z. Lu, J. Tribol. 142 (2020) 1.
[38] G. Tatsumi, M. Ratoi, Y. Shitara, K. Sakamoto, B.G. Mellor, Tribol. Int. 151 (2020), 106513.
[39] Y. Yamamoto, M. Hashimoto, Wear 253 (2002) 820.
[40] M. Minn, S.K. Sinha, Wear 296 (2012) 528.
[41] A. Kurdi, H. Wang, L. Chang, Tribol. Int. 117 (2018) 225.
[42] S. Bahadur, Wear 245 (2000) 92.
[43] T. Yamaguchi, K. Hokkirigawa, Tribol. 11 (2016) 653.
[44] C.S. Wu, E.E. Klaus, J.L. Duda, J. Tribol. 111 (1989) 121.
[45] N.A. Wright, S.N. Kukureka, Wear 250–251 (2001) 1567.
[46] P. Rycerz, A. Kadiric, Tribol. Lett. 67 (2019) 1.
[47] X. Li, B. Bhushan, Mater. Char. 48 (2002) 11.
[48] T. Iqbal, B.J. Briscoe, P.F. Luckham, Eur. Polym. J. 47 (2011) 2244.
[49] G.Z. Voyiadjis, A. Samadi-Dooki, L. Malekmotiei, Polym. Test. 61 (2017) 57.
[50] A. Avanzini, G. Donzella, A. Mazzù, C. Petrogalli, Tribol. Int. 57 (2013) 22.
[51] A. Schallamach, Wear 1 (1958) 384.
[52] M. Bonne, B.J. Briscoe, C.J. Lawrence, S. Manimaaran, D. Parsonage, A. Allan, Tribol. Lett. 18 (2005) 125.
[53] J.W.M. Mens, A.W.J. de Gee, Wear 149 (1991) 255.
[54] A. Wang, S. Yan, B. Lin, X. Zhang, X. Zhou, Friction 5 (2017) 414.
[55] T. Kunishima, Y. Nagai, T. Kurokawa, G. Bouvard, J.C. Abry, V. Fridrici, P. Kapsa, Wear (2020) 456–457.
[56] B.J. Hamrock, D. Dowson, NASA Tech. Note (1976) D-8317.
[57] B.J. Hamrock, D. Dowson, NASA Tech. Note (1977) D-8528.
[58] N. Marx, J. Guegan, H.A. Spikes, Tribol. Int. 99 (2016) 267.
[59] M. Zalaznik, M. Kalin, S. Novak, Tribol. Int. 94 (2016) 92.
[60] G. Zhang, Z. Rasheva, A.K. Schlarb, Wear 268 (2010) 893.